

SCIENTIFIC REPORTS



OPEN

Ultrafast Intrinsic Photoresponse and Direct Evidence of Sub-gap States in Liquid Phase Exfoliated MoS₂ Thin Films

Received: 16 October 2014

Accepted: 15 May 2015

Published: 15 July 2015

Sujoy Ghosh¹, Andrew Winchester¹, Baleeswaraiiah Muchharla¹, Milinda Wasala¹, Simin Feng², Ana Laura Elias², M. Bala Murali Krishna³, Takaaki Harada³, Catherine Chin³, Keshav Dani³, Swastik Kar⁴, Mauricio Terrones^{2,5} & Saikat Talapatra^{1,3}

2-Dimensional structures with swift optical response have several technological advantages, for example they could be used as components of ultrafast light modulators, photo-detectors, and optical switches. Here we report on the fast photo switching behavior of thin films of liquid phase exfoliated MoS₂, when excited with a continuous laser of $\lambda = 658$ nm ($E = 1.88$ eV), over a broad range of laser power. Transient photo-conductivity measurements, using an optical pump and THz probe (OFTP), reveal that photo carrier decay follows a bi-exponential time dependence, with decay times of the order of picoseconds, indicating that the photo carrier recombination occurs via trap states. The nature of variation of photocurrent with temperature confirms that the trap states are continuously distributed within the mobility gap in these thin film of MoS₂, and play a vital role in influencing the overall photo response. Our findings provide a fundamental understanding of the photo-physics associated with optically active 2D materials and are crucial for developing advanced optoelectronic devices.

Single- and few-layers of atomically thin Molybdenum Disulfide (MoS₂) possess fascinating and unprecedented physico-chemical properties¹. Along with attractive values of carrier mobilities, the possibility of achieving a current saturation in these materials indicate their potential use as thin film transistors and light emitting diodes². Monolayer MoS₂ is a direct band gap semiconductor (~ 1.8 eV) in contrast to its bulk counterpart (n-type semiconductor with an indirect band gap of ~ 1.3 eV), and therefore can be viewed as a valuable candidate for fabrication of components in electronic or optoelectronic devices³⁻⁷. Kim *et al.*³ have shown that by properly choosing the dielectric substrate, it is possible to attain high room temperature mobilities as well as very low sub threshold swing in few layer MoS₂ field effect transistors. In addition, single and few layers of MoS₂ exhibit impressive optical properties related to tunable photo detection^{5,6}. These findings have resulted in the search for innovative methods related to the synthesis of MoS₂ flakes of controlled thickness⁸⁻¹⁵. Methods such as laser thinning¹¹, Chemical vapor deposition (CVD)^{5,16,17} and liquid phase exfoliation⁸ are now routinely used to obtain atom-thick layers of MoS₂.

Among these techniques, liquid phase exfoliation such as the one reported by Coleman *et al.*⁸ is considered to be the most suitable method for achieving large scale and low cost synthesis of few layer MoS₂.

¹Department of Physics, Southern Illinois University Carbondale, Carbondale-IL 62901. ²Department of Physics and Center for 2-Dimensional and Layered Materials, The Pennsylvania State University, University Park, PA 16802. ³Femtosecond Spectroscopy Unit, Okinawa Inst. of Science & Technology, Graduate University, Onnason, Okinawa, 904 -0495 Japan. ⁴Department of Physics and George J. Kostas Research Institute, Northeastern University, Boston, USA. ⁵Department of Chemistry and Department of Materials Science and Engineering, The Pennsylvania State University, University Park, PA 16802. Correspondence and requests for materials should be addressed to S.T. (email: stalapatra@physics.siu.edu) or S.G. (email: sujoy.kittu@siu.edu)

Since these materials are directly exfoliated in suspensions, they can be used as inks and can be used to cast thin films on a variety of substrates without any additional processing or transferring. In this letter we demonstrate that thin films of such liquid phase exfoliated MoS₂ (see Methods for exfoliation details) can be used as photo-detectors with ultrafast photo-carrier generation and recombination times. These detectors can offer responsivity values of $\sim 10^{-4}$ AW⁻¹, higher than the responsivity values reported for CVD grown WS₂ flakes^{16,17}. Optical pump and Terahertz probe (OPTP) measurements indicate that the decay in the conductivity of the photo carriers closely follows a bi-exponential time dependence with a fast decay component $\tau_1 \sim 5$ ps and a slower component $\tau_2 \sim 110$ ps. The slower decay component is a manifestation of electron-hole recombination in trap states (recombination centers) present between the valence band and the conduction band. We predict that these trap states are continuously distributed throughout the mobility gap of the photo-detector device. This prediction is made on the basis of photocurrent (I_{ph}) measurements performed at low light power levels ($20 \mu\text{W} < P < 570 \mu\text{W}$, $\lambda = 633$ nm), which show that I_{ph} increases as a fractional power of light intensity over a broad range of temperature, a signature of continuous distribution of trap states¹⁸. In order to understand the role of these trap states in controlling the photocurrent behavior, temperature dependence of I_{ph} at a low light power of $\sim 570 \mu\text{W}$ ($\lambda = 633$ nm) was measured. We observed that I_{ph} increased with decreasing temperature (from 330 K to 280 K) and reaches a maximum value at $T = T_m \sim 80$ K. Thereafter I_{ph} decreases with further decrease in temperature, becoming greater than the dark current at ~ 120 K, and finally becomes temperature independent below 50 K. Such behavior is explained on the basis of the availability of trap states (acting as recombination centers) with the variation of temperature, and aligns well with established models of photo-carrier recombination processes in disordered semiconductors.

In Fig. 1 spectroscopy and microscopy characterization of the exfoliated MoS₂ flakes are presented. A few droplets of the exfoliated MoS₂ dispersion (Fig. 1a) were deposited and dried on SiO₂ and analyzed by Raman spectroscopy. Raman measurements using the 514 nm laser excitation line (Renishaw Raman Spectrometer; Fig. 1b) were collected from several positions of the deposited film. A detailed analysis performed on the collected Raman measurements from the film and comparing it with on the available literature indicates that the exfoliated MoS₂ flakes contain more than 4 layers (see supplementary information).

In Fig. 1c, we show the Tauc analysis of the UV-Vis spectra obtained from the MoS₂ dispersions (details are provided in the supplementary section), which indicate that the dispersions possess an optical gap of ~ 1.74 eV. High Resolution Transmission Electron Microscopy (HRTEM) images of typical flakes are depicted in Fig. 1d–h. HRTEM images of the edges of some of these flakes (Fig. 1g,h) reveal the presence of multiple layers. These flakes were deposited on inter-digitated platinum electrodes (with a separation of 5 μm between two electrodes—see supplementary information for details of electrodes used.) on borosilicate glass substrates in order to form a thin film photo-detector. The MoS₂ thin films deposited on the electrodes were then annealed at $\sim 150^\circ\text{C}$ for 2 hours (in an argon flow of 500 sccm) in order to improve the contact resistance between the MoS₂ flakes and the electrodes. Finally, the electrodes were mounted inside a close cycle Helium cryostat (Janis Model # SHI- 4-1) with optical windows and pumped to high vacuum ($\sim 10^{-5}$ Torr) before performing the photoconduction measurements.

Room temperature current vs. voltage (IV) measurements without and with laser illumination was performed (using a Keithley Source meter 2400 Series) in order to investigate the nature of photoconduction in the device. A Coherent Cube solid-state laser system with a wavelength $\lambda = 658$ nm ($E = 1.88$ eV), 60 mW maximum power output and with a circular spot size of 3 mm diameter was used to illuminate the samples. The results of room temperature photoresponse investigation on these films are presented in Fig. 2a. The linear IV response with *light off* and *light on* under forward and reverse bias conditions and the absence of any zero-bias photocurrent in our devices (see supplementary information) indicate little or no photovoltaic contribution due to barrier effects occurring at the contacts, and thus the photoconduction is attributed to the photo carrier generation within the bulk portion of the MoS₂ film. In order to investigate the photo switching behavior of the device at different light intensities, a 2 V DC bias was applied across the two terminals of the device and the corresponding current passing through the device without laser illumination (dark current; I_{dark}) and with laser illumination (current under illumination; I_{ill}) was recorded. Laser illumination of the device was switched ON and OFF in roughly 1000 ms intervals with varying laser output power from 0.67 mW to 60 mW. This data is presented in Fig. 2b. Fast photo switching of the detector on the order of ≤ 100 ms was observed, and it is of the similar order as previously reported in the case of single-layer MoS₂ phototransistors⁵. In order to determine the intrinsic photo-carrier recombination times, instantaneous transient THz conductivity in exfoliated MoS₂ films was measured using OPTP, described in detail later.

Along with the fast photo switching of these thin film photodetectors, a non-linear dependence of light intensity on I_{ill} was observed. We found that the photocurrent ($I_{ph} = I_{ill} - I_{dark}$) follows a power dependence following $I_{ph} \sim P^\gamma$, where P is laser intensity with $\gamma = 0.66$ (Fig. 2c). This behavior is different for simple crystals which typically possess $\gamma = 0.5$, corresponding to bimolecular processes, or $\gamma = 1$, corresponding to monomolecular processes. The monomolecular and bimolecular recombination processes are the two extreme cases observed in simple crystalline semiconducting systems with few trap states. We would like to note that several processes could lead to nonlinear power dependence of photocurrent. For example, photo-gating artifacts, thermoelectric effects, trapping by mid-gap states etc. comprise such processes. Our detailed investigations (described later in the manuscript) related to the variation of the

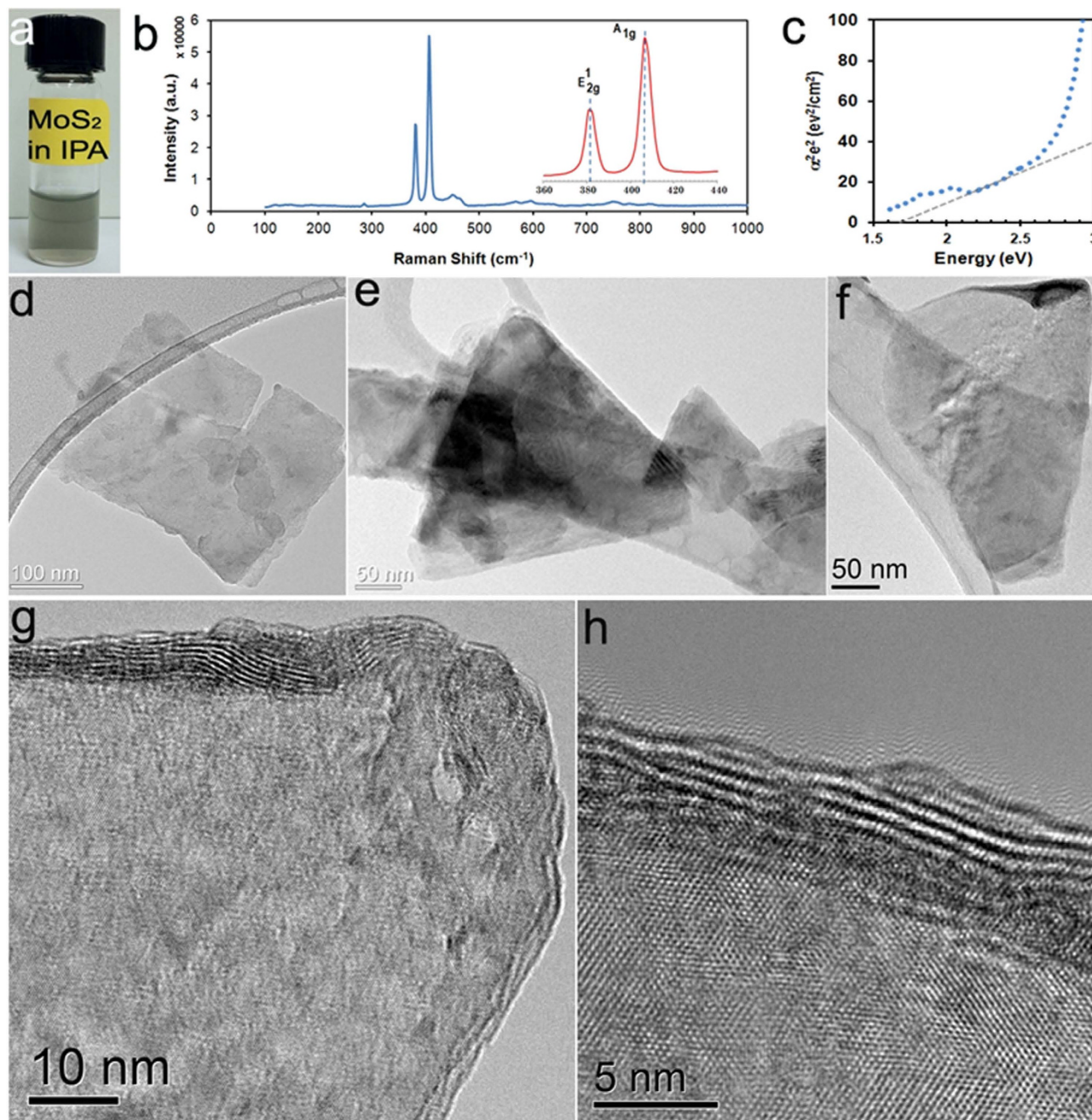


Figure 1. Synthesis and characterization of liquid phase exfoliated MoS₂. (a) Digital image of exfoliated MoS₂ dispersion in IPA. (b) Raman spectra measured from the samples. (c) Tauc plot extracted from the UV-Vis spectrum of the exfoliated samples. (d) (e) & (f) TEM images of typical flakes. (g) & (h) shows the HRTEM images of exfoliated flakes showing few layers as well as a highly crystalline structure.

power exponent with temperature as well as the comparative behavior of dependence of dark current and photocurrent with temperature strongly suggests that the photoconduction phenomenon in our films are similar to those obtained in the case of disordered semiconductor. Nevertheless, in order to verify that photo gating effects are not contributing to any photocurrent in our devices we have measured photocurrent by impinging the laser spot on the substrate in close proximity of the electrodes covered with MoS₂ film. The device was then slowly moved under the laser illumination, such that the laser spot traversed from one end of the bare substrate over the device to the other end of the bare substrate (please refer to supplementary figure S8). The current response from the device was measured throughout this process. We found that an increase in current was only observed when the laser spot was on the sample, indicating that absorption of light in the substrate or by charges that reside near the device does not cause any changes in the photocurrent. Further, we have also noted that the photocurrent decay are fast, without

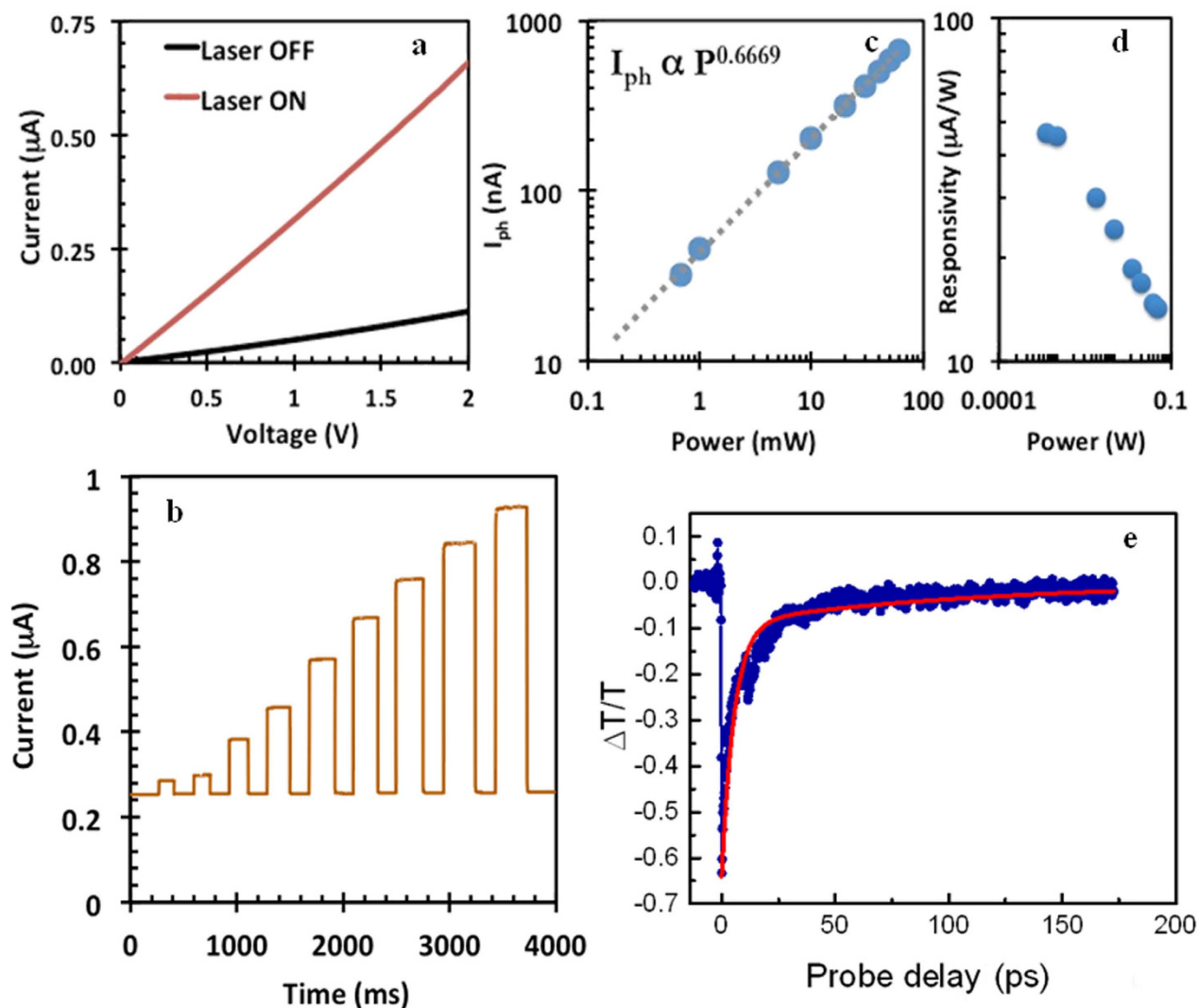


Figure 2. Electrical and optical measurements on liquid phase exfoliated MoS₂ films. (a) IV measurement on MoS₂ device, with light off and light on (b) photo switching at ~283 K for (from left to right) 0.67, 1, 5, 10, 20, 30, 40, 50 and 60 laser power (in mW). (c) Variation of I_{ph} with laser intensity (at 60 mW). (d) Detector responsivity as a function of laser power. (e) Transient Differential THz Transmission proportional to photoconductivity ($\Delta T/T \sim \Delta\sigma$) measurement as a function of probe delay time, showing a bi-exponential decay in photoconductivity (fit solid line).

any prolonged photocurrent decay tail (which arises if significant thermal effects are present), which suggests that contributions from thermoelectric effects are perhaps negligible. These observations leads us to believe that the fractional power dependence of photocurrent with laser intensity seen is indicative of the presence of a large number of trap states within these films¹⁸ (as explained in detail later).

We have also evaluated the responsivity and external quantum efficiency of these samples at different laser powers. Responsivity is defined as $\mathcal{R} = I_{ph}/P_{light}$ (where P_{light} is the power of the incident light)⁵, and is an important performance parameter of any photo detector. Figure 2d shows the responsivity of the exfoliated MoS₂ films measured at different laser power with an applied bias of 2 V. The responsivity at the lowest power (0.67 mW) was found to be $\sim 50 \mu A W^{-1}$ with a corresponding external efficiency of $\sim 10^{-2}\%$. This low external quantum efficiency is due to the highly disordered nature of the film. By increasing the applied bias to 20 V and the laser excitation power to 60 mW, a responsivity of $\mathcal{R} \sim 0.1 mA W^{-1}$ can be obtained (supplementary information). However this is significantly lower than the reported values for single- and few-layered MoS₂ FET devices^{5,6}, but is considerably higher than multilayer WS₂ based devices¹⁶. Further, these \mathcal{R} values are also similar to the values obtained on exfoliated MoS₂/ITO junction photodetectors¹⁷.

As mentioned earlier, the fractional light intensity dependence of the photocurrent is due to the presence of trap states in the exfoliated MoS₂ film. We provide further evidence of the presence of these trap states by measuring the photo carrier decay dynamics using OPTP. For this purpose, a ~70 femtosecond, 400 nm, 1kHz pump pulse with a fluence of 0.8 mJ/cm² was used to photo excite electron and hole pairs in ~2.5 mm diameter spot in these films. A sub-picosecond THz probe pulse, derived from the same laser system, was generated using optical rectification in a ZnTe nonlinear crystal (see supplementary information for schematic of the measurement setup). The instantaneous transient THz conductivity of the photo-carriers ($\Delta\sigma$) was measured by recording the change in transmission of the peak of the THz pulse ($\Delta T/T$) as a function of pump probe delay. In general, for thin films, $\Delta\sigma \sim -\Delta T/T$ ¹⁹. Thus, the generation of mobile photo-carriers results in a decrease in transmission of the THz peak, i.e. a negative OPTP signal, which eventually recovers to zero as the carriers lose mobility due to trapping or recombination.

In our measurements, carriers were measured as a function of the pump probe delay. We found that the decay in conductivity of the photo-carriers follows a bi-exponential time dependence with a fast decay component $\tau_1 \sim 5$ ps, and a slower decay component $\tau_2 \sim 110$ ps, indicating the presence of multiple relaxation processes (Fig. 2e). The time scales observed in our samples are similar to those found in the case of photo excited carrier relaxation times of mechanically cleaved single and few layers of MoS₂ crystals, where the fast initial decay time τ_1 (~few ps) is a signature of photo carriers being trapped by trap states²⁰ and the longer decay time τ_2 (~few hundreds of ps) is manifestation of photo carrier recombination. The dynamics of the photo carriers, which ultimately determines the performance of these materials in developing optical devices with ultrafast response times, depends on the distribution and nature of these trap states in the forbidden zone. The presence of sub-gap trap states are often found in thin films of exfoliated 2-D materials, for example reduced Graphene Oxide (rGO) films where the transport mechanism is mediated through a Mott-type variable-range hopping across sub-gap energy values²¹. Since few-layered MoS₂ is a material of high importance in the next-generation of optoelectronic devices, understanding the nature of these sub-gap states is of vital importance from fundamental as well as applied perspectives. An understanding of the distribution of trap states as well as the availability of trap states in the photo conduction process is therefore necessary, and this can be determined by systematically monitoring the temperature dependence of the power exponent γ ²² and by studying the temperature dependence of I_{ph} at fixed low light intensities²³.

In order to understand the distribution of the trap states in the MoS₂ photo detectors, we have performed measurements of I_{ph} at very low light intensities and at different temperatures. For this purpose a Uniphase Helium Neon Gas Laser ($\lambda = 633$ nm, $E = 1.95$ eV) with a maximum power output of 1mW was used. The results are depicted in Fig. 3. First, we confirmed the photo response of the device by applying a DC bias of 500 mV under a laser illumination power of 575 μ W at various temperatures. The photo response under such conditions is presented in Fig. 3a. The dependence of I_{ph} on the laser power P (20μ W $< P < 575 \mu$ W) again showed fractional power dependence of the form $I_{ph} \sim P^\gamma$ (Fig. 3b) with $0.5 < \gamma < 1.0$ over a broad range of temperatures. A similar dependence of photocurrent is typically observed in a wide variety of disordered semiconductors and can be explained by the existence of a large number of trap states between the valence and conduction bands^{18,23}. The disordered nature of the film therefore should give rise to a large number of localized trap states in the mobility gap. These trap states, which lie between the conduction band and the steady state Fermi level for electrons ((SSFL)_n), do not take part in the recombination process since electrons falling into these states are rapidly re-excited thermally into the conduction band. A similar reasoning is also applied to trap states which lie between the valence band and steady state Fermi level for holes ((SSFL)_p). However, the states lying between the SSFLs are responsible for recombination of electrons or holes. These states are designated as recombination centers; the free charge carriers falling into these states will generally recombine and will not contribute to the conduction. Under these assumptions, once the excitation is increased (for example by increasing the laser intensity), the number of free carriers increase and the two steady-state Fermi levels move apart toward their respective band edges, increasing the number of recombination centers (a phenomenon also known as electronic doping)²⁴. The increase in the number of recombination centers reduces the lifetimes of the free carriers, thereby causing a sub-linear dependence of photocurrent on the incident light intensity values, which is what has been observed in our measurements. A simple schematic showing this process is represented in Fig. 3d.

Furthermore, the nature of the distribution of the trap states could be determined from the temperature dependence of γ . In particular, Haynes *et al.* have shown²⁵ that it is possible to predict the distribution of the localized states by monitoring the value and temperature dependence of γ at low laser powers. For example, it is noted that a temperature dependence of the form $\gamma = T_c/(T + T_c)$, where T_c is a characteristic temperature, indicates that the trap states are perhaps distributed exponentially. Our measurements indicate values of γ ranging between 0.5 and 1.0, over a wide range of temperature (30 K $< T < 220$ K), and follow a similar temperature dependence when $T_c \cong 300$ K (see Fig. 3c). In general the dependence of γ on temperature, as seen in our measurement, is strongly associated with a continuous distribution of trap states of the form $\sim \exp(-\Delta E/KT)$ below the conduction band, where ΔE is the energy separation measured from the bottom of the conduction band¹⁸. Therefore, we can confirm that in few-layered MoS₂ thin film photo detectors, the trap states are continuously distributed.

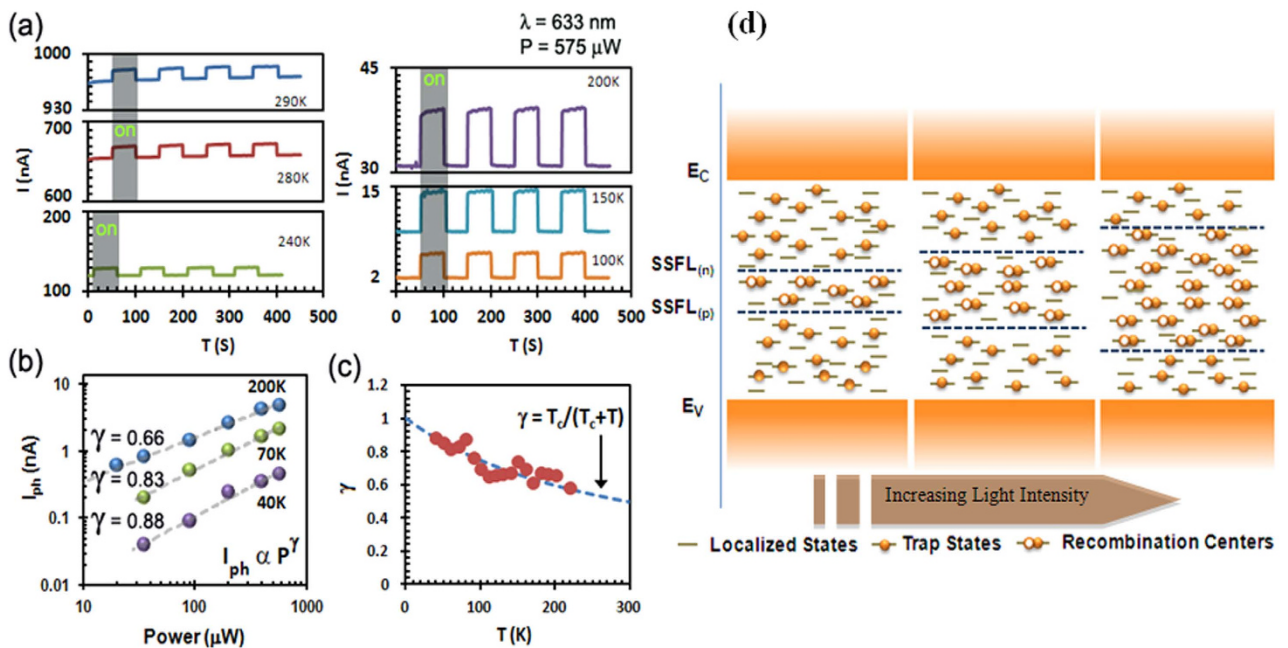


Figure 3. Temperature dependence of optical properties of liquid phase exfoliated MoS₂ films. (a) The photo response of the device measured (applied voltage 1 V, $\lambda = 633$ nm, $P = 575 \mu\text{W}$) at several temperatures is presented. (b) Dependence of photocurrent with respect to low light intensity on the same device (applied voltage 0.5 V, $\lambda = 633$ nm) (c) Temperature dependence of power exponent γ under low light condition. (d) Schematic representation of the movement of Steady State Fermi Levels with increases light intensity.

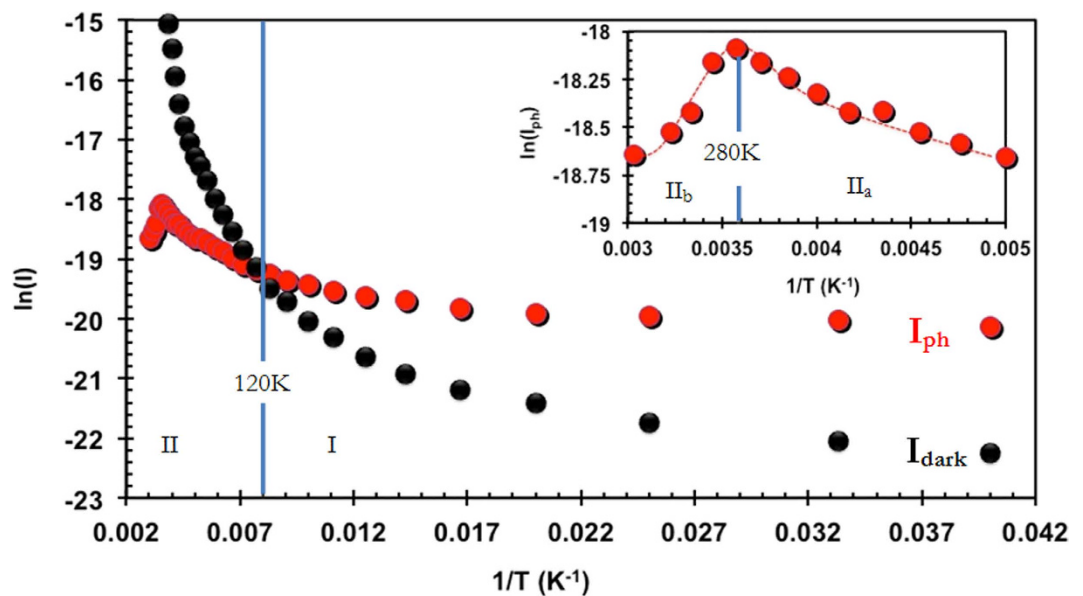


Figure 4. Temperature dependence of photocurrent. Temperature dependence of photocurrent and dark current as seen in thin film MoS₂ photo-detectors. A maximum of photocurrent at high temperatures (inset) as well as higher value of photocurrent compared to dark current at lower temperatures.

In order to understand how the trap states control the photocurrent of these devices over a wide range of temperature, we have measured the dependence of I_{ph} with temperature ($25 \text{ K} < T < 320 \text{ K}$) by applying a DC bias of 500 mV, under a constant illumination ($\lambda = 633$ nm, $E = 1.95$ eV) at $575 \mu\text{W}$. The data is presented in Fig. 4, where $\ln(I_{\text{ph}})$ is plotted as a function of $1/T$ and it is compared with the value of I_{dark} . Several interesting features of I_{ph} can be seen from this measurement. Firstly, depending on the measurement temperatures, two distinct regions for I_{ph} can be identified: Region I ($T < 120 \text{ K}$; where $I_{\text{ph}} >$

I_{dark}) and Region II ($T > 120$ K; where $I_{\text{ph}} < I_{\text{dark}}$). Secondly, at low temperatures ($T < 50$ K), I_{ph} is constant and thirdly, in Region II ($T > 120$ K), I_{ph} shows a maxima at $T = T_{\text{max}} \sim 280$ K.

These behaviors can be understood by considering the position of the SSFLs as described under the model proposed by Rose¹⁸. At low temperatures (Region I, $T < 120$ K) the SSFLs are closer to each other (away from their respective band edges). Under these conditions, in our system, the number of photo-generated carriers (N_{ph}) is significantly greater than the number of trap states acting as recombination centers (N_{rc}). This leads to the condition where $I_{\text{ph}} > I_{\text{dark}}$. At sufficiently low temperatures ($T \leq 50$ K), a constant I_{ph} is also observed, indicating that a constant photo carrier density is reached in these photo detectors. As the temperature increases, the two SSFLs move apart toward their respective band edges, thus increasing the number of recombination centers. Under these conditions, $N_{\text{rc}} \gg N_{\text{ph}}$ and thus higher recombination of the generated photo carriers occur, resulting in I_{ph} becoming $< I_{\text{dark}}$ (as seen in region II ($T \geq 120$ K)). Further in this region, I_{ph} shows a maxima at $T = T_{\text{max}} \sim 280$ K (Inset Fig. 4). In the past, it has been shown for several photoactive disordered semiconductors that although the photo current on both sides of T_{max} is carried through extended states, as the temperature increases (for $T > T_{\text{max}}$) the number of thermally generated carriers also increase²⁶. This in turn increases the dark current and results in the decrease of I_{ph} once T_{max} is reached.

In conclusion we have shown that films of few-layered liquid phase exfoliated MoS₂ are suitable candidates for fabricating fast response photo detectors. Detailed photocurrent measurements as a function of temperature show that these films contain extended trap states, which mainly arise due to the disorder caused by the random orientation of the stacked layers of the exfoliated flakes. This results in a faster recombination of the charge carriers, but also reduces the responsivity of these materials when compared to several recently studied mechanically exfoliated and Chemical Vapor Transport grown 2D layered chalcogenides^{27–35}. However, we have also shown that under certain conditions, responsivities higher than few layer CVD grown WS₂ photo detectors is possible, but overall improvements in responsivity by further tuning the exfoliation process could be reached in the future. A table (supplementary information) detailing the responsivity of several single and few layer Chalcogenides is also presented for comparison. One important aspect of these findings is directly related to the fabrication of low-cost photo-detectors or electrode materials for low-loss solar power conversion. In order to optimize the performances of such devices, a clear understanding of the photo carrier dynamic and the role of sub gap states present in these materials is essential. We believe that the experimental evidence related to the inherent presence of sub gap states in liquid-phase exfoliated 2D MoS₂ flakes sheds light on several aspects of their photo response behavior. The results presented in this manuscript will not only open up similar investigations, but also will motivate the development of photoactive nano-materials and composites for several opto-electronic applications.

Methods

The synthesis of MoS₂ dispersions was performed via a liquid phase exfoliation technique described by Coleman *et al.*⁸. Commercial MoS₂ powder (Sigma Aldrich, $< 2 \mu\text{m}$) was added to isopropanol alcohol (IPA) at a concentration ratio of 10 mg/mL. The mixture was then treated with ultrasound from a Fisher Scientific Sonic Dismembrator 500 horn tip sonicator operating between 20% to 40% amplitude. The dispersions were treated with ultrasound for 4 hours continuously, using an ice water bath to maintain the temperature. After the ultrasound treatment, the dispersions were centrifuged at 1500 rpm for 45 minutes and were then decanted. The dispersion thus obtained was used to fabricate the photo detector device. This was achieved by depositing a small droplet of the dispersion containing the exfoliated MoS₂ on pre-fabricated inter-digitated electrode assembly with inter-digitated finger separation of $5 \mu\text{m}$ (ALS Japan). The devices were then annealed at 150°C under an Argon atmosphere for 2 hours. Annealing leads to the reduction in the amount of chemical impurities, surface ad-atoms etc. present in the samples due to the exfoliation process thereby making the metal sample interface less resistive. A schematic of the whole process is shown in the supplementary information. After the annealing the device was mounted on a closed cycle Helium Cryostat (Janis Model SHI) and was pumped down (pressures typically below 10^{-5} Torr) overnight before performing optical measurements.

References

1. Radisavljevic, B., Radenovic, A., Brivio, J., Giacometti, V. & Kis, A. Single-layer MoS₂ transistors. *Nat. Nanotechnol.* **6**, 147–150 (2011).
2. Wang, Q. H., Kalantar-Zadeh, K., Kis, A., Coleman, J. N. & Strano, M. S. Electronics and optoelectronics of two-dimensional transition metal dichalcogenides. *Nat. Nanotechnol.* **7**, 699–712 (2012).
3. Kim, S. *et al.* High-mobility and low-power thin-film transistors based on multilayer MoS₂ crystals. *Nat. Commun.* **3**, 1011 (2012).
4. Zhang, Y., Ye, J., Matsushashi, Y. & Iwasa, Y. Ambipolar MoS₂ thin flake transistors. *Nano Lett.* **12**, 1136–40 (2012).
5. Yin, Z. *et al.* Single-layer MoS₂ phototransistors. *ACS Nano* **6**, 74–80 (2012).
6. Lee, H. S. *et al.* MoS₂ nanosheet phototransistors with thickness-modulated optical energy gap. *Nano Lett.* **12**, 3695–3700 (2012).
7. Eda, G. *et al.* Photoluminescence from chemically exfoliated MoS₂. *Nano Lett.* **11**, 5111–5116 (2011).
8. Coleman, J. N. *et al.* Two-dimensional nanosheets produced by liquid exfoliation of layered materials. *Science* **331**, 568–571 (2011).
9. Smith, R. J. *et al.* Large-scale exfoliation of inorganic layered compounds in aqueous surfactant solutions. *Adv. Mater.* **23**, 3944–3948 (2011).

10. Björkman, T., Gulans, A., Krashennnikov, A. V. & Nieminen, R. M. Van der Waals bonding in layered compounds from advanced density-functional first-principles calculations. *Phys. Rev. Lett.* **108**, 235502 (2012).
11. Castellanos-Gomez, A. *et al.* Laser-thinning of MoS₂: On demand generation of a single-layer semiconductor. *Nano Lett.* **12**, 3187–3192 (2012).
12. Zhan, Y., Liu, Z., Najmaei, S., Ajayan, P. M. & Lou, J. Large-area vapor-phase growth and characterization of MoS₂ atomic layers on a SiO(2) substrate. *Small* **8**, 966–71 (2012).
13. Lee, Y.-H. *et al.* Synthesis of large-area MoS₂ atomic layers with chemical vapor deposition. *Adv. Mater.* **24**, 2320–5 (2012).
14. Liu, K. K. *et al.* Growth of large-area and highly crystalline MoS₂ thin layers on insulating substrates. *Nano Lett.* **12**, 1538–1544 (2012).
15. Winchester, A. *et al.* Electrochemical characterization of liquid phase exfoliated two-dimensional layers of molybdenum disulfide. *ACS Appl. Mater. Interfaces* **6**, 2125–2130 (2014).
16. Perea-López, N. *et al.* Photosensor Device Based on Few-Layered WS₂ Films. *Adv. Funct. Mater.* **23**, 5511–5517 (2013).
17. Cunningham, G. *et al.* Photoconductivity of solution-processed MoS₂ films. *J. Mater. Chem. C* **1**, 6899 (2013).
18. Rose, A. Recombination processes in insulators and semiconductors. *Phys. Rev.* **97**, 322–333 (1955).
19. Nuss, M. C. & Orenstein, J. *Millimeter and Submillimeter Wave Spectroscopy of Solids* [Grüner, G. (ed.)] [7–50] (Springer, Berlin, 1998).
20. Shi, H. *et al.* Exciton dynamics in suspended monolayer and few-layer MoS₂ 2D crystals. *ACS Nano* **7**, 1072–1080 (2013).
21. Muchharla, B., Narayanan, T. N., Balakrishnan, K., Ajayan, P. M. & Talapatra, S. Temperature dependent electrical transport of disordered reduced graphene oxide. *2D Mater.* **1**, 011008 (2014).
22. Halpern V. The intensity dependence of the steady-state photoconductivity in amorphous semiconductors. *J. Phys. C Solid State Phys.* **21**, 2555–2563 (1988).
23. Rose, A. *Concepts in photoconductivity and allied problems.* (Interscience Publishers, New York, 1963).
24. Kao Kwan Chi. *Dielectric Phenomena in Solids.* (Academic Press, Burlington, 2004).
25. Haynes, J. R. & Hornbeck, J. A. Temporary traps in silicon and germanium. *Phys. Rev.* **90**, 152–153 (1953).
26. Mott, N. F. & Davis, E. *Electronic Processes in Non-crystalline Materials.* (Oxford University Press, London, 1971).
27. Lopez-Sanchez, O., Lembke, D., Kayci, M., Radenovic, A. & Kis, A. Ultrasensitive photodetectors based on monolayer MoS₂. *Nat. Nanotechnol.* **8**, 497–501 (2013).
28. Hu, P. *et al.* Highly responsive ultrathin GaS nanosheet photodetectors on rigid and flexible substrates. *Nano Lett.* **13**, 1649–1654 (2013).
29. Choi, W. *et al.* High-detectivity multilayer MoS₂ phototransistors with spectral response from ultraviolet to infrared. *Adv. Mater.* **24**, 5832–5836 (2012).
30. Jacobs-Gedrim, R. B. *et al.* Extraordinary photoresponse in two-dimensional In₂Se₃ nanosheets. *ACS Nano* **8**, 514–521 (2014).
31. Liu, F. *et al.* High-sensitivity photodetectors based on multilayer GaTe flakes. *ACS Nano* **8**, 752–760 (2014).
32. Hu, P., Wen, Z., Wang, L., Tan, P. & Xiao, K. Synthesis of few-layer GaSe nanosheets for high performance photodetectors. *ACS Nano* **6**, 5988–5994 (2012).
33. Lei, S. *et al.* Synthesis and photoresponse of Large GaSe Atomic Layers. *Nano Lett.* **13**, 2777–2781 (2013).
34. Lei, S. *et al.* Evolution of the electronic band structure and efficient photo-detection in atomic layers of InSe. *ACS Nano* **8**, 1263–1272 (2014).
35. Island, J. O. *et al.* Ultrahigh Photoresponse of Few-Layer TiS₃ Nanoribbon Transistors. *Adv. Opt. Mater.* **2**, 641–645 (2014).

Acknowledgment

This work is supported by the U.S. Army Research Office through a MURI grant # W911NF-11-1-0362. SK acknowledges the funding support provided by US National Science Foundation through NSF ECCS CAREER Award # 1351424 and partial support from the US Army under grant W911NF-10-2-0098, sub award 15-215456-03-00. ST & KMD acknowledges the funding support provided by US National Science Foundation (NSF) through grant # NSF-PIRE OISE-0968405 and Japan Society for the Promotion of Science (JSPS).

Author Contributions

S.G., S.K. and S.T. conceived and designed the project. S.G., B.M., M.W. and S.T. performed the low temperature electrical transport and photo-transport measurements and analyzed the data. A.W., S.G., B.M. and M.W. synthesized MoS₂ using liquid phase exfoliation method. A.W. and M.W. performed and analyzed the Uv-Vis measurements. S.F., A.E. and M.T. performed and analyzed Raman spectroscopy and HRTEM. M.K., T.H., C.C. and K.D. performed and analyzed the OPTP measurements. All authors contributed to the writing of the manuscript.

Additional Information

Supplementary information Detail information regarding UV-Vis, Raman and HRTEM are provided. Additional information regarding electrical and optical characterization of these materials is also discussed. Supplementary information accompanies this paper at <http://www.nature.com/srep>

Competing financial interests: The authors declare no competing financial interests.

How to cite this article: Ghosh, S. *et al.* Ultrafast Intrinsic Photoresponse and Direct Evidence of Sub-gap States in Liquid Phase Exfoliated MoS₂ Thin Films. *Sci. Rep.* **5**, 11272; doi: 10.1038/srep11272 (2015).



This work is licensed under a Creative Commons Attribution 4.0 International License. The images or other third party material in this article are included in the article's Creative Commons license, unless indicated otherwise in the credit line; if the material is not included under the Creative Commons license, users will need to obtain permission from the license holder to reproduce the material. To view a copy of this license, visit <http://creativecommons.org/licenses/by/4.0/>